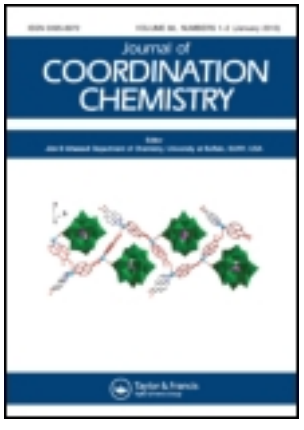

Journal of Coordination Chemistry
Publication details, including instructions for authors and subscription information:
http://www.tandfonline.com/loi/gcoo20

Complexation studies of Cm(III), Am(III), and Eu(III) with linear and cyclic carboxylates and polyaminocarboxylates

Punam Thakur [a c], James L. Conca [b] & Gregory R. Choppin [a]

[a] Department of Chemistry and Biochemistry, Florida State University, Tallahassee, FL 32306-4390, USA

[b] MSA Analytical Services, RJ Lee Group, Inc., Richland, WA 99352, USA

[c] Carlsbad Environmental Monitoring and Research Center, 1400 University Drive, Carlsbad, NM 88220, USA

Published online: 14 Sep 2011.

To cite this article: Punam Thakur, James L. Conca & Gregory R. Choppin (2011) Complexation studies of Cm(III), Am(III), and Eu(III) with linear and cyclic carboxylates and polyaminocarboxylates, Journal of Coordination Chemistry, 64:18, 3214-3236, DOI: 10.1080/00958972.2011.616927

To link to this article: http://dx.doi.org/10.1080/00958972.2011.616927

Journal of Coordination Chemistry
Vol. 64, No. 18, 20 September 2011, 3214–3236

Complexation studies of Cm(III), Am(III), and Eu(III) with linear and cyclic carboxylates and polyaminocarboxylates

PUNAM THAKUR†§*, JAMES L. CONCA‡ and GREGORY R. CHOPPIN†

†Department of Chemistry and Biochemistry, Florida State University, Tallahassee, FL 32306-4390, USA
‡MSA Analytical Services, RJ Lee Group, Inc., Richland, WA 99352, USA
§Carlsbad Environmental Monitoring and Research Center, 1400 University Drive, Carlsbad, NM 88220, USA

(*Received 14 February 2011; in final form 1 August 2011*)

Solvent extraction and potentiometric titration methods have been used to measure the stability constants of Cm(III), Am(III), and Eu(III) with both linear and cyclic carboxylates and polyaminocarboxylates in an ionic strength of 0.1 mol L^{-1} ($NaClO_4$). Luminescence lifetime measurements of Cm(III) and Eu(III) were used to study the change in hydration upon complexation over a range of concentrations and pH values. Aromatic carboxylates, phthalate (1,2 benzene dicarboxylates, PHA), trimesate (1,3,5 benzene tricarboxylates, TSA), pyromellitate (1,2,4,5 tetracarboxylates, PMA), hemimellitate (1,2,3 benzene tricarboxylates, HMA), and trimellitate (1,2,4 benzene tricarboxylates, TMA) form only 1 : 1 complexes, while both 1 : 1 and 1 : 2 complexes were observed with PHA. Their complexation strength follows the order: PHA∼TSA > TMA > PMA > HMA. Carboxylate ligands with adjacent carboxylate groups are bidentate and replace two water molecules upon complexation, while TSA displaces 1.5 water molecules of hydration upon complexation. Only 1 : 1 complexes were observed with the macrocyclic dicarboxylates 1,7-diaza-4,10,13-trioxacyclopentadecane-N,N′-diacetate (K21DA) and 1,10-diaza-4,7,13,16-tetraoxacyclooctadecane-N,N′-diacetate (K22DA); both 1 : 1 and 1 : 2 complexes were observed with methyleneiminodiacetate (MIDA), hydroxyethyleneiminodiacetate (HIDA), benzene-1,2-bis oxyacetate (BDODA), and ethylenediaminediacetate (EDDA), while three complexes (1 : 1, 1 : 2, and 1 : 3) were observed with pyridine 2,6 dicarboxylates (DPA) and chelidamate (CA). The complexes of M-MIDA are tridentate, while that of M-HIDA is tetradentate in both 1 : 1 and 1 : 2 complexes. The M-BDODA and M-EDDA complexes are tetradentate in the 1 : 1 and bidentate in the 1 : 2 complexes. The complexes of M-K22DA are octadentate with one water molecule of hydration, while that of K21DA is heptadentate with two water molecules of hydration. Simple polyaminocarboxylate 1,2 diaminopropanetetraacetate (PDTA) and ethylenediamine N,N′-diacetic-N,N′-dipropionate (ENDADP) like ethylenediaminetetraacetate (EDTA) form only 1 : 1 complexes and their complexes are hexadentate. Polyaminocarboxylates with additional functional groups in the ligand backbone, e.g., ethylenebis(oxyethylenenitrilo) tetraacetate (EGTA), and 1,6 diaminohexanetetraacetate (HDTA) or with additional number of groups in the carboxylate arms diethylenetriamine pentaacetato-monoamide (DTPA-MA), diethylenetriamine pentaacetato-bis-methoxyethylamide (DTPA-BMEA), and diethylenetriamine pentaacetato-bis glucosaamide (DTPA-BGAM) are octadentate with one water molecule of hydration, except N-methyl MS-325 which is heptadentate with two water molecules of hydration and HDTA which is probably dimeric with three water molecules of hydration. Macrocyclic tetraaminocarboxylate, 1,4,7,10-tetraazacyclododecanetetraacetate (DOTA) forms only 1 : 1 complex which is octadentate with one water molecule of hydration. The functionalization of these carboxylates and polycarboxylates affect the complexation ability toward metal cations. The results, in

*Corresponding author. Email: pthakur@cemrc.org

Journal of Coordination Chemistry
ISSN 0095-8972 print/ISSN 1029-0389 online
DOI: 10.1080/00958972.2011.616927

conjunction with previous results on the Eu(III) complexes, provide insight into the relation between ligand steric requirement and the hydration state of the Cm(III) and Eu(III) complexes in solution. The data are discussed in terms of ionic radii of the metal cations, cavity size, basicity, and ligand steric effects upon complexation.

Keywords: Complexation; Luminescence; Cm(III); Am(III); Eu(III)

1. Introduction

The coordination chemistry of actinides and lanthanides, especially interactions with organic ligands expected in the repository, has attracted great attention to better understand their behavior in waste media, and predicting the migration behavior of actinides in the environment. Carboxylate and aminocarboxylates, some of which were widely used in nuclear material processing and cleanup/decontamination processes and are of importance in waste processing, form fairly strong complexes with Ln and An (f-elements) cations. The interaction of Ln and An with these ligands has been extensively studied in terms of stability constants and thermodynamics, but there is still much to be learned about the structure and composition of the coordination spheres of these complexes [1, 2].

The inner sphere hydration number of a metal ion complex provides important information on the structural properties of the species present in solution. Although recent sophisticated techniques such as extended X-ray absorption fine structure (EXAFS), X-ray diffraction, and nuclear magnetic resonance (NMR) relaxation measurements have been used for direct determination of the coordination number of lanthanide and actinide complexes, the easy availability, high sensitivity, and selectivity of time resolved laser induced fluorescence spectroscopy (TRLFS) makes it the most promising direct method for measurement of the hydration number of radioactive cations, such as Cm(III) and Am(III). Beitz and Hessler [3] reported the first lifetime measurement study of Cm(III) in aqueous solution, while recently Bernhard *et al.* [4] reported the first fluorescence lifetime measurement study of Am(III)-pyromellitic complex. Since then several groups have studied the spectroscopy and fluorescence of Cm(III) complexes and compared the results with earlier research [5]. Because of its relatively long half-life and high fluorescence efficiency, ^{248}Cm(III) has been studied as an analog for other An(III) ions in a variety of systems by TRLFS [5]. However, compared to Eu(III) and Tb(III) spectroscopy which has been studied extensively, such studies on the application of Cm(III) or Am(III)-TRLFS as a speciation method are relatively few, probably because of the scarcity of ^{248}Cm and the weak luminescence intensity and much shorter lifetime of Am(III) ($Am^{3+}_{(aq)} = 27.2$ ns) [4] in comparison with Cm(III) ($Cm^{3+}_{(aq)} = 64\,\mu s$) [6].

The inner sphere hydration number, N_{H_2O}, of the trivalent lanthanides varies from 9 to 8 as the atomic number increases [7]. A similar trend is expected for the trivalent actinide ions. For Cm^{3+} ($Z = 96$), $N_{H_2O} = 9$ has been reported from luminescence lifetime measurements [6] and confirmed by crystallographic and EXAFS structural studies [8]. Like Eu(III) and Tb(III), a linear correlation has been found for Cm(III) between the decay constant, k_{obs} and N_{H_2O} in the inner coordination sphere of their complexes [7]. Rao *et al.* [9] studied hydration of Cm(III) in aqueous solution as a function of temperature. The weak temperature dependency of lifetime and intensity

suggests that Cm(III) aqua ion remains as $Cm(H_2O)_9^{3+}$ in the H_2O–D_2O system from 10°C to 85°C. In the TRLFS study, from 20°C to 200°C [10] the fluorescence lifetime of the Cm(III) aqua ion was temperature dependent, suggesting that the correlation between lifetime and the hydration number of Cm(III) previously reported in the literature [6] may be applicable only to room temperature solutions.

The high sensitivity of TRLFS of Cm(III) allows study of its complexation reactions over a wide range of concentrations and pH values [11]. Luminescence has been used extensively in the studies of interactions of Cm(III) with bio-organic molecules [12, 13], with inorganic and organic ligands [5, 14], with iso- and hetero-polyoxoanions (i.e., $W_{10}O_{36}^{12-}$, $P_2W_{17}O_{31}^{10-}SiW_{11}O_{39}^{8-}$ [15]) and with mineral phases [5]. In this article, we report the stability constants of Cm(III) and Am(III) with carboxylate and polyaminocarboxylate ligands, and the hydration number of the chemical species formed between these cations and ligands using Eu(III) and Cm(III) luminescence in solution. Previous studies used Eu(III) or Tb(III)-luminescence to elucidate the structure of Cm(III) complexes. In this research, Cm(III)-luminescence was used to measure the hydration of Cm(III) in such complexes. A broad category of linear and cyclic carboxylates and polyaminocarboxylates were chosen in this study on the basis of their chelate ring size, basicity, ligand donors etc., to obtain an understanding of the role of these parameters on actinide complexation and hydration state. The functionalization of ligands either by inserting additional groups in the ligand backbone or by inserting additional groups in the carboxylate arm introduces new properties into a ligand; it can make it more selective toward a metal ion, it can increase the thermodynamic stability and the kinetic inertness, and it can change the solubility and extractability into an organic phase. Since the properties of f-element metal ion complexes are determined principally by ionic and steric effects, comparison of the complexation of these ligands provides insight into the role of different donor groups and how the steric differences between the ligands affects the complexation strength.

2. Experimental

All chemicals were reagent grade and distilled; deionized water was used for solution preparation. Solutions of 2.0 mol L^{-1} sodium perchlorate (99.99% Sigma-Aldrich, ACS certified) were prepared in deionized water and filtered through a 0.45 μm membrane to maintain the desired ionic strengths. Solutions of carboxylates, picolinate (PA), picolinate N-oxide (PAO), phthalate (1,2 benzene dicarboxylates, PHA), trimellitate (1,2,4 benzene tricarboxylates, TMA), hemimellitate (1,2,3 benzene tricarboxylates, HMA), pyromellitate (1,2,4,5 tetracarboxylates, PMA), trimesate (1,3,5 benzene tricarboxylates, TSA), methyleneiminodiacetate (MIDA), hydroxyethyleneiminodiacetate (HIDA), benzene-1,2-bis(oxyacetate) (BDODA), ethylenediaminediacetate (EDDA), 1,7-diaza-4,10,13-trioxacyclopentadecane-N,N′-diacetate (K21DA), 1,10-diaza-4,7,13,16-tetraoxacyclooctadecane-N,N′-diacetate (K22DA), pyridine 2,6 dicarboxylates (DPA), piperidine 2,6 dicarboxylate (PDA), chelidamate (CA), and of aminopolycarboxylates 1,2 diaminopropanetetracetate (PDTA), ethylenebis(oxyethylenenitrilo) tetraacetate (EGTA), 1,4,7,10-tetraazacyclododecanetetraacetate (DOTA), ethylenediamine N,N′-diacetic-N,N′-dipropionate (ENDADP), 1,6 diaminohexanetetraacetate (HDTA), diethylenetriamine pentaacetato-monoamide (DTPA-MA),

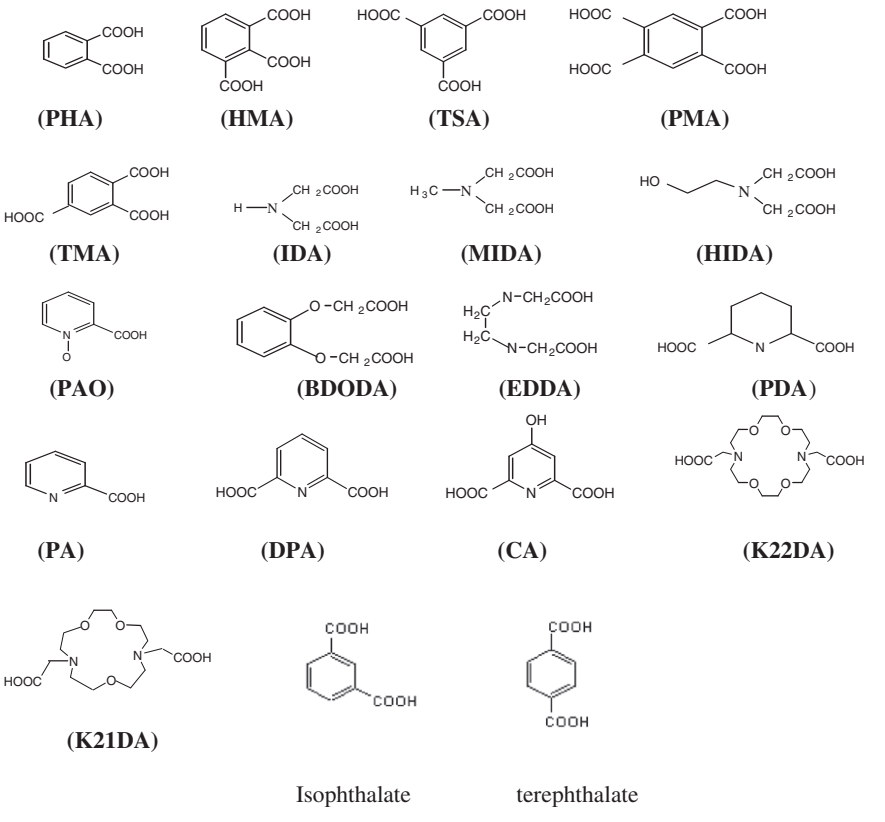

Scheme 1. Schematic diagram of the ligands.

diethylenetriamine pentaacetato-bis-methoxyethylamide (DTPA-BMEA), and diethylenetriamine pentaacetato-bis glucosaamide (DTPA-BGAM) were prepared and standardized by potentiometric titration with carbonate free NaOH solution. The structures of the ligands used and/or discussed are shown in schemes 1 and 2. The ligands PDA, DOTA, DTPA-MA, and DTPA-BMEA were gift samples either from Mallinckrodt or Argonne National Laboratory. DTPA-BGAM was synthesized by Schaab [16]. Measurements of pH were performed with a Fisher Accumet 950 pH meter equipped with a Corning Semi-Micro combination electrode filled with saturated sodium chloride solution. The pH meter was calibrated at pH 4.00 and 7.00 using Fisher buffer solutions. The hydrogen ion concentration, pcH, was calculated from the measured pH reading using the relation $pcH = pHr + 0.259(\pm 0.025) \times C_{NaClO_4}$ (where C = concentration of $NaClO_4$). The calibration curves were obtained by a series of measurements of $HClO_4$ and NaOH solutions of known H^+ concentrations for $I = 0.1$–$5.0\,mol\,L^{-1}$ ($NaClO_4$) at room temperature.

2.1. *Preparation of ^{248}Cm solution for excitation study*

^{248}Cm was purified by passage through a column of Dowex-1 anion exchange resin in $7.5\,mol\,L^{-1}$ HNO_3. The collected Cm fraction was evaporated to dryness and

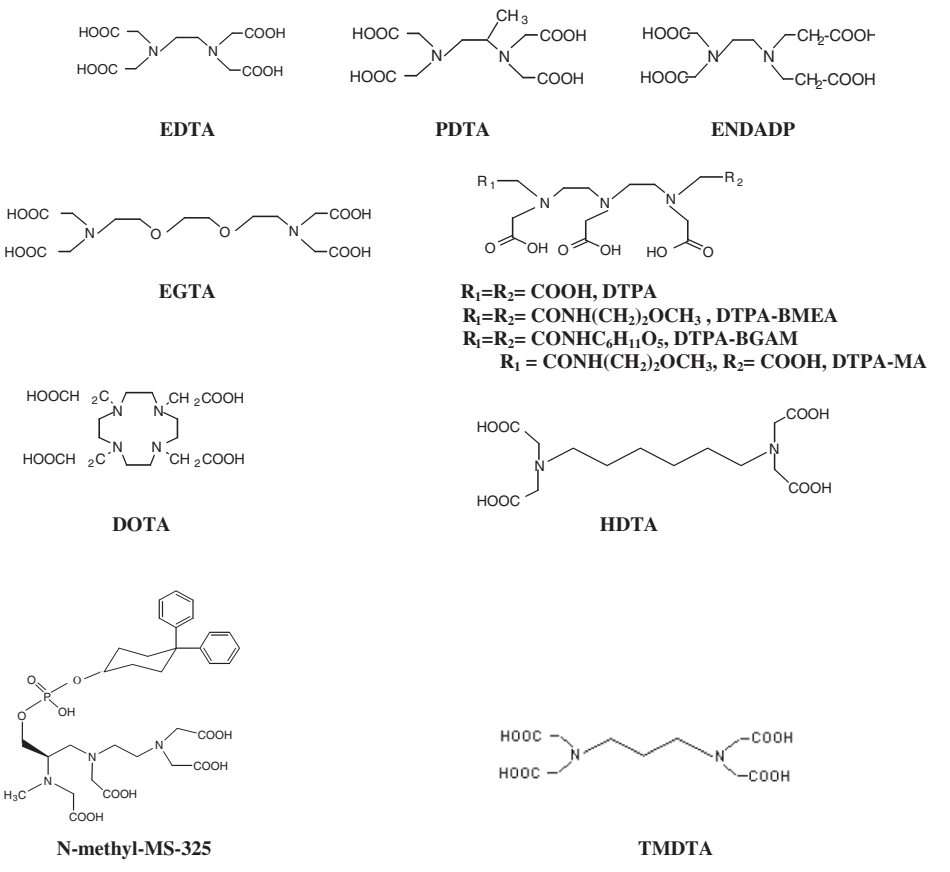

Scheme 2. Schematic diagram of the ligands.

redissolved in 0.001 mol L^{-1} $HClO_4$. The concentration of Cm^{3+} stock solution was determined by α-spectrometry and liquid scintillation counting. The Eu^{3+} stock solution was prepared from Eu_2O_3 (99.99%, Aldrich) in perchloric acid and the concentration determined by EDTA titration using xylenol orange as indicator.

2.2. *Measurement of excitation spectra*

Excitation spectra of the Cm(III) complexes in a standard 1.0 cm quartz cell were obtained by scanning the dye laser spectrum of the $^8S_{7/2} \rightarrow {}^6I_{17/2,\ 11/2}$ band, while monitoring the luminescence emission intensity at 600 nm to measure the luminescence lifetime. Details of the instrumental setup were as described [6, 14]. The excitation was achieved with a pulsed (10 Hz) 532 nm beam of an Nd-YAG laser (Quanta Ray DCR 3 A, Spectra-Physics) pumping DCM (Exciton Inc.) in methanol solution in a Quanta Ray PDL 2 (Spectra-Physics) dye laser head. The laser beam was converted to the desired wavelength (388–410 nm range) by mixing the dye laser output with the 1064 nm

fundamental in a wavelength extender module (Quanta Ray WEX-1). Eu(III) excitation spectra were recorded by scanning the tunable dye laser stepwise at regular wavelength intervals through the absorption band (577.7–580.7 nm), while monitoring the emission of $^7F_0 \rightarrow {}^5D_0$ at 616 nm [17]. The deconvolution of the excitation spectra was performed using Lorentzian–Gaussian functions. The concentration of Cm(III) was $2.0–4.0 \times 10^{-6}$ mol L^{-1}, while that of Eu(III) was 1.0×10^{-4} mol L^{-1}.

Lifetime measurements were performed at a fixed wave number corresponding to the maxima of the fluorescence peak intensity of each spectrum. Fluorescence decay curves were collected using a LeCroy 9410 Dual 150 MHz oscilloscope. The data were transferred to a computer using software supplied with the oscilloscope (NEWSCOPE). The software had been modified by Dr van de Burgt. The lifetime of the fluorescence decay of the various Cm(III) and Eu(III) species was fitted with the mono-exponential decay equation.

The correlations $N_{H_2O} = 0.65k_{obs} - 0.88$ and $N_{H_2O} = 1.05k_{obs} - 0.70$ [6, 18], where k_{obs} is the luminescence decay constant, were used to calculate the number of water molecules associated with Cm(III) and Eu(III), respectively. An uncertainty of ± 0.5 is assigned to the N_{H_2O} values in these measurements [14, 18].

2.3. *Solvent extraction procedure*

Tracers ^{241}Am, ^{244}Cm, and $^{152,\ 154}$Eu obtained from Oak Ridge National Laboratory were used for the solvent extraction studies. The radiochemical purity of the tracer was checked by α- and/or γ-spectrometry. ^{244}Cm was purified from its daughter nuclide ^{240}Pu in the same way as ^{248}Cm. The working stock of the tracer was prepared in a solution of pcH = 3.0 ($HClO_4$) with an activity of *ca* 50,000 counts per minute (cpm) per 10.0 μL. The activities of ^{241}Am, ^{244}Cm, and $^{152,\ 154}$Eu were counted with a Beckman Liquid Scintillation Counter (LSC) using Ecolite cocktail (ICN, Research Product Division).

Solvent extraction experiments were conducted in 20 mL liquid scintillation vials at a fixed volume ratio of 3.0 mL organic : 3.0 mL aqueous solution. All extraction experiments were performed at a fixed pH 3.60 ± 0.05. The organic solutions (5×10^{-4} mol L^{-1} D2EHPA/heptane for Cm(III) and Am(III) and 2×10^{-4} mol L^{-1} for Eu(III)) were pre-equilibrated with the aqueous stock solutions. The aqueous solutions of the reaction mixture were 0.1 mol L^{-1} ($NaClO_4$), with or without ligands. A 20.0 μL (*ca* 60,000 cpm) volume of the radioactive tracer solution were added into each vial and the vials were shaken in a water bath (Cole-Parmer Inst. Co., Polystat Model 1200-00 circulator) at 180 rpm for 1 h at 25.0 ± 0.1°C, which had been determined to be sufficient time to ensure equilibrium for all the systems. After equilibrium was reached, the vials were centrifuged for 3–5 min, 0.50–1.0 mL of duplicate samples were taken from both phases and the activities were counted in a Beckman Liquid Scintillation Counter (LSC) by mixing aliquots of the samples with approximately 10 mL Ecolite (ICN, Research Product Division) liquid scintillation cocktail. The remaining aqueous phase was used for measurement of the equilibrium pH. The error calculations for the stability constants are expressed as 95% confidence limits based upon two or three determinations. In the extraction experiment, the pH of the aqueous phase sometimes

varied slightly after contact with the organic phase. When necessary, the measured D values were corrected using the equation:

$$\log D_{\text{corr}} = \log D - n \times (\text{pcH} - \text{pcH}_{\text{av}}), \quad (1)$$

where D is the distribution ratio, pcH_{av} is the average pcH for each experiment and n is the value of the experimental slope of the $\log D_0$ *vs.* pcH plot in the absence of the ligand, which was measured to be 2.93 for Cm(III), 2.89 for Am(III), and 2.85 for Eu(III). This correction usually did not exceed 5–10% of the D value for each sample.

For distribution measurement in the presence of complexing ligands, the concentrations of the ligand were varied from 0.01 to 0.08 mol L^{-1} for PHA, 0.01 to 0.025 mol L^{-1} for TMA and PMA, 0.008 to 0.018 mol L^{-1} for HMA, 0.002 to 0.006 mol L^{-1} for TSA, 0.02 to 0.08 mol L^{-1} for MIDA, 0.001–0.008 mol L^{-1} for K21DA and K22DA, 1.0×10^{-4} to 5×10^{-4} mol L^{-1} for BDODA, HIDA, PDTA and ENDADP, 0.25 to 5.0×10^{-5} mol L^{-1} for EGTA, 1.0×10^{-7} to 6.0×10^{-7} mol L^{-1} for DTPA, DTPA-MA, DTPA-BMEA, DTPA-BGAM and N-methyl MS-325.

2.4. *Potentiometric titration*

Potentiometric titrations were conducted in a 50 mL jacketed cell controlled to $\pm 0.1^{\circ}$C with an isotemp Model 910 constant temperature circulator. The cell was capped with a jacketed lid to minimize condensation and volume loss during titration of the solution. The titrant solution was delivered by a Metrohm Dosimat 665 motor-driven piston burette. Nitrogen was bubbled through the titration solution to remove dissolved carbon dioxide. The titrations were performed with stirring on a Corning model PC420 stirrer/hot plate. The system was interfaced to a computer that operated software prepared in the laboratory to control burette additions and to record the mV reading of the electrode. The delay between the readings was $\geq$30 s to assure equilibrium. After the addition was made, the system waited a mixing time, typically 30 s, before restarting the measurement cycle. Prior to each titration or complexation titration, the electrode was calibrated by an acid–base titration using standardized perchloric acid and sodium hydroxide solutions at the desired temperatures so that hydrogen ion concentrations could be calculated from the emf readings in subsequent titrations.

The ligand and metal solutions, usually in the ratio of 1 : 1 or 1 : 2 (15 mL of 0.003–0.010 mol L^{-1} in 0.1 mol L^{-1} $NaClO_4$), were titrated automatically by an incremental addition of standardized 0.1000 mol L^{-1} NaOH from the burette over a pcH range from 2 to 11, collecting 120 data points per titration. The titration data were fitted by PSEQUAD and HYPERQUAD to calculate the acid dissociation constants and the stability constants [19, 20]. The value of pK_w was fixed at 13.78 for all analyses. The titration curve for Eu-CA at 1 : 2 ratio is shown in figure 1.

2.5. *Calculation of stability constant*

The extraction of M^{3+} between the aqueous phase and the organic phase with D2EHPA, represented as the dimer (H_2A_2) can be expressed as

$$M^{3+}_{(a)} + 3H_2A_{2(o)} \Leftrightarrow M(HA_2)_{3(o)} + 3H^{+}_{(a)}, \quad (2)$$

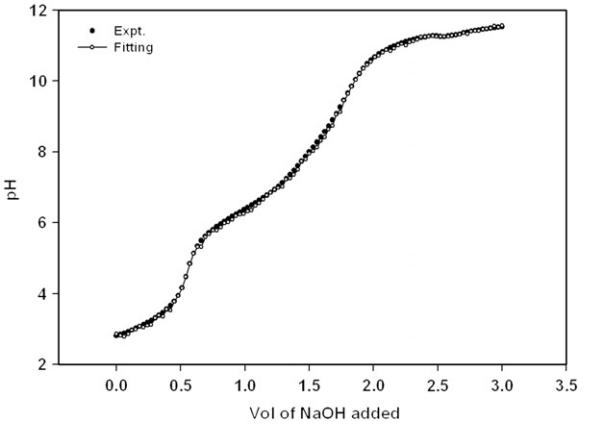

Figure 1. Titration curve for formation of Eu(III)-CA, $I = 0.1\,\text{mol}\,\text{L}^{-1}$ ($NaClO_4$), Eu(III) : CA = 1 : 2, $T = 25^{\circ}\text{C}$.

where subscripts (a) and (o) represent the aqueous and organic phases, respectively. In the presence of L^{m-} in the aqueous phase, the complexation reaction of the metal ions can be written as

$$M^{3+} + nL^{m-} \Leftrightarrow ML_n^{(3-nm)}. \tag{3}$$

A linear curve of $1/D$ (D = distribution ratio = $[M^{3+}]_{\text{total,(o)}}/[M^{3+}]_{\text{total,(a)}}$) *vs.* $[L^{m-}]$ for the metal ion indicates the presence of a 1 : 1 complex, while a nonlinear curve indicates the formation of more than one complex. The stability constants (β_{101} and β_{102}) of the complexes formed were evaluated using the polynomial

$$D_0/D - 1 = \beta_{101}[L^-] + \beta_{102}[L^-]^2, \tag{4}$$

where D_0 is the distribution ratio in the absence of ligand, $[L^-]$ is the free ligand concentration calculated from the equilibrium pcH, the total ligand concentrations,and the relevant protonation constants. The first stability constant, β_{101} was calculated as a slope of the linear regression between $(D_0/D - 1)$ and the free ligand concentration $[L^-]$ using the first five data points for solvent extraction. The second stability constant, β_{102} was calculated as the slope of the linear regression between $(D_0/D - 1)/[L^-]$ and $[L^-]$. Equal weight was given to each data point. All reported errors are uncertainties at the 95% ($\pm 2\sigma$) confidence level.

3. Results and discussion

Luminescence lifetimes and the corresponding number of water molecules, N_{H_2O}, in the aqueous complex of Cm(III) and Eu(III) and of the binary complexes with carboxylates are listed in table 1. The excitation peak of $Cm(III)_{(aq)}$ in $I = 0.1\,\text{mol}\,\text{L}^{-1}$ ($NaClO_4$) appears at 396.70 nm with a lifetime of $64 \pm 5\,\mu\text{s}$ and $N_{H_2O} = 9.1$ which agree with

Table 1. TRLFS data of the Cm(III) and Eu(III) with carboxylates; $[Cm(III)] = 2.0–4.0 \times 10^{-6}$ mol L^{-1}, $[Eu(III)] = 1.0 \times 10^{-4}$ mol L^{-1}; $T = 25°C$, $I = 0.1$ mol L^{-1} ($NaClO_4$).

Component	Ratio	pH	Excitation (nm)	Species	Lifetime (μs)	N_{H_2O} (±0.5)
Cm(aq)	–	2.5	396.70	–	64 ± 3	9.1
Eu(aq)	–	2.2	578.90	–	113 ± 5	8.6
Cm-PHA	1 : 800	6.0	397.36	$Cm(PHA)^+$	86 ± 7	6.7
Eu-PHA	1 : 10	5.0	579.03	$Eu(PHA)^+$	142 ± 7	6.8
	1 : 20	6.0	579.30	$Eu(PHA)_2^-$	–	–
Cm-TMA	1 : 800	6.0	397.45	Cm(TMA)	88 ± 4	6.5
Eu-TMA	1 : 10	5.0	–	Eu(TMA)	141 ± 5	6.8
Cm-HMA	1 : 800	5.9	397.61	Cm(HMA)	84 ± 5	6.9
Eu-HMA	1 : 10	5.8	579.03	Eu(HMA)	143 ± 5	6.7
Cm-PMA	1 : 800	5.8	397.30	$Cm(PMA)^-$	82 ± 3	7.0
Eu-PMA	1 : 10	6.0	17271	$Eu(PMA)^-$	143 ± 4	6.7
Cm-TSA	1 : 800	5.9	397.24	Cm(TSA)	77 ± 4	7.5
Eu-TSA	1 : 10	5.8	578.99	Eu(TSA)	132 ± 5	7.3

previous reports [6, 14]. The excitation spectrum of $Eu(III)_{(aq)}$ shows a peak at 578.90 nm with a lifetime of 113 ± 5 μs and $N_{H_2O} = 8.6$.

The stability constants of Cm(III) and Am(III) with aromatic carboxylates PHA, HMA, PMA, TMA, and TSA measured by solvent extraction are listed in table 2. Linear plots of $1/D$ *vs.* $[L]^{m-}$ indicate formation of 1 : 1 complex; figure 2(a) is a representative graph for Cm-PMA and Cm-HMA. The stability constants of Cm(III) and Am(III) determined in this work are in good agreement with those reported for the Eu(III) complexes with these ligands [17]. The high stability values of HMA and PMA as compared to PHA can be attributed to the statistical effect of having multiple bidentate sites on the tri- and tetracarboxylates in contrast to the single bidentate site on phthalate. Figure 3 shows the relationship between the stability constant *versus* the total ligand basicity, ΣpK_a. Deviation of the values for isophthalate (1,3-benzene dicarboxylates), trimesate, hemimellitate, and pyromellitate complexes can be explained by considering the arrangement of the donor groups in these ligands. Isophthalate and trimesate anions bind the metal only by a single carboxylate and have, respectively, two and three possible binding sites. Similarly, tri-, hemi-, and pyromellitate anions are bidentate, which gives each ligand two sets of possible binding sites. The calculated N_{H_2O} values of the complexes (table 1) indicate that complexation of Cm(III) with the aromatic carboxylates PHA, HMA, PMA, and TMA displaces two water molecules, while displacement of *ca* 1.5 water molecules of hydration by TSA indicates that this ligand interacts partially in bidentate fashion or that steric hindrance causes displacement of extra water molecules of hydration from the inner coordination shell of the metal cations.

Linear plots of $1/D$ *versus*. $[L]^{m-}$ are also observed for L = MIDA, HIDA, and BDODA, consistent with the presence of the 1 : 1 complex (figure 2(b), a representative graph for Cm-MIDA). The stability constant values measured are listed in table 2. The formation of 1 : 2 complexes was not observed in our studies; however, these dicarboxylates are known to form complexes higher than 1 : 1 with these cations at high concentration and pH. The complexation strength follows the order: HIDA > EDDA > IDA (iminodiacetate) ≈MIDA > BDODA (table 2), consistent with

Table 2. Stability constants of Am(III), Cm(III), and Eu(III) with linear and cyclic carboxylates and polyaminocarboxylates at $I = 0.1\,\text{mol}\,L^{-1}$ ($NaClO_4$); $T = 25°C$.

Ligands	Method	Am(III)	Cm(III)	Eu(III)	Ref.
PHA	sx	3.75 ± 0.03	3.84 ± 0.04	3.70 ± 0.03	p.w
	lif	–	–	3.45 ± 0.02	[17]
TMA	sx	4.55 ± 0.06	4.48 ± 0.05	4.32 ± 0.04	p.w
	lif	–	–	4.19 ± 0.10	[17]
PMA	sx	5.42 ± 0.05	5.35 ± 0.03	4.98 ± 0.03	p.w
	lif	–	–	5.81 ± 0.04	[17]
HMA	sx	5.68 ± 0.05	5.64 ± 0.04	5.08 ± 0.03	p.w
	lif	–	–	5.25 ± 0.01	[17]
TSA	sx	3.76 ± 0.03	3.62 ± 0.04	3.70 ± 0.03	p.w
	lif	–	–	3.56 ± 0.10	[17]
BDODA	sx	5.24 ± 0.05	5.10 ± 0.04	5.02 ± 0.03	p.w
MIDA	sx	7.52 ± 0.06	7.69 ± 0.04	7.45 ± 0.05	p.w
				6.92	[22]
HIDA	sx	10.30 ± 0.06	9.98 ± 0.07	9.69 ± 0.05	p.w
		9.14	9.14	9.10	[22]
IDA		6.90	–	6.73	[22]
EDDA		–	–	8.38	[22]
DPA	Pot*	8.52 ± 0.04	8.32 ± 0.05	8.15 ± 0.05	p.w
		15.05 ± 0.05	15.15 ± 0.04	14.98 ± 0.04	
CA	Pot*	7.85 ± 0.03	7.62 ± 0.03	7.52 ± 0.03	p.w
		13.95 ± 0.05	14.15 ± 0.05	14.56 ± 0.05	
K21DA	sx	12.06 ± 0.06	11.98 ± 0.05	11.62 ± 0.06	p.w
	pot	12.86 ± 0.03**	–	11.85	[35]
K22DA	sx	13.60 ± 0.05	13.47 ± 0.06	12.76 ± 0.05	p.w
		13.33 ± 0.11**	–	12.02	[35]
ENDADP	sx	13.84 ± 0.06	14.01 ± 0.07	13.77 ± 0.05	p.w
PDTA	sx	17.85 ± 0.06	17.92 ± 0.05	17.75 ± 0.07	p.w
HDTA	sx	10.09 ± 0.04	10.12 ± 0.05	9.36 ± 0.04	p.w
EGTA		17.980 ± 0.09	17.940 ± 0.09	17.65 ± 0.08	p.w
DOTA	sx	23.95 ± 0.09	24.02 ± 0.11	23.95 ± 0.10	p.w
		–	–	23.5	[36]
DTPA-BMEA	sx	16.30 ± 0.06	16.58 ± 0.04	16.35 ± 0.05	p.w
		–	–	16.48	[16]
DTPA-BGAM	sx	15.9 ± 0.05	15.78 ± 0.06	16.02 ± 0.05	p.w
		–	–	16.0	[16]
DTPA-MA	sx	18.48 ± 0.06	18.56 ± 0.05	18.95 ± 0.06	p.w
N-MS-325	sx	20.12 ± 0.08	20.08 ± 0.06	20.17 ± 0.07	p.w

Pot = potentiometry; sx = solvent extraction; lif = laser induced fluorimetry.
* = log β_{102}; ** = sx.

increased number of donor atoms in HIDA and EDDA (4) compared to MIDA and IDA (3 in both complexes).

The luminescence lifetime data indicate formation of 1 : 1 and 1 : 2 complexes for MIDA, HIDA, and EDDA (table 3), but only the 1 : 1 complex for BDODA in our experimental conditions. From the N_{H_2O} values (table 3), it can be concluded that HIDA is tetradentate and MIDA is tridentate in the 1 : 1 and 1 : 2 complexes. In the case of BDODA and EDDA, the 1 : 1 complex is tetradentate, while 1 : 2 complex is bidentate, indicating that extra groups in the ligands produced steric hindrance which prevents tetradentate coordination in the 1 : 2 complexes [21]. The NMR shift data of Ln-BDODA (Ln^{3+} = Pr, Eu, and Yb) are consistent with tetradentate coordination of BDODA in the 1 : 1 complex binding *via* two ether oxygen atoms (Ln–O = 2.20 Å) and

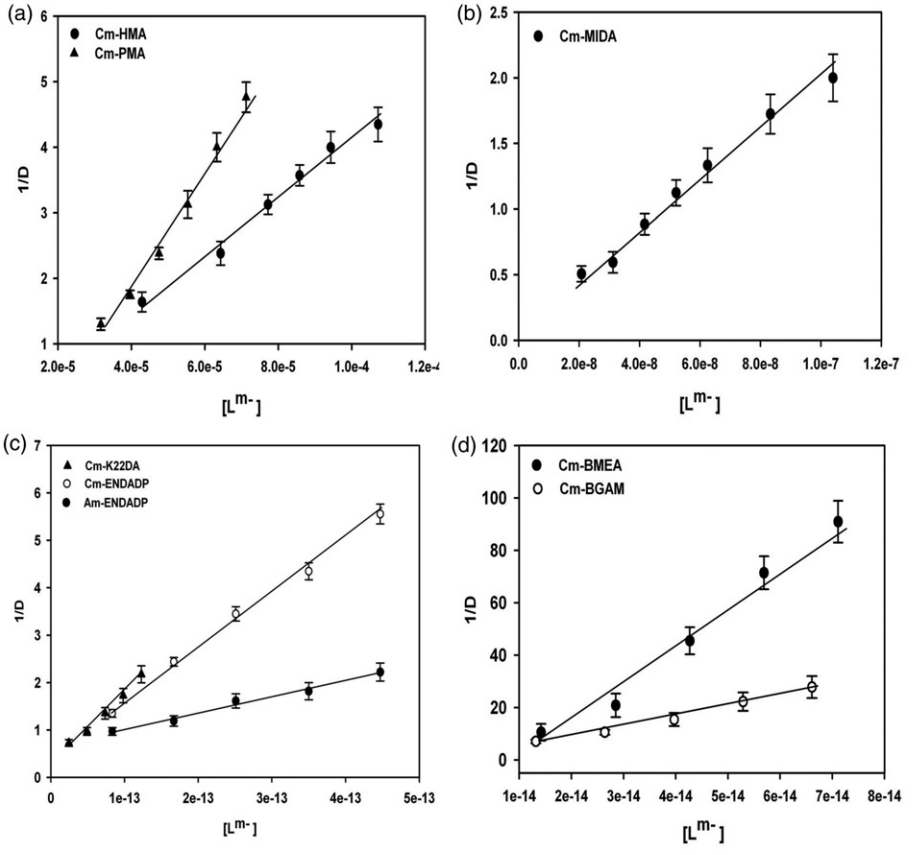

Figure 2. The variation of $1/D$ for Am(III) and Cm(III) as a function of free ligand concentration at an ionic strength of 0.1 mol L^{-1} ($NaClO_4$) and $T = 25°C$.

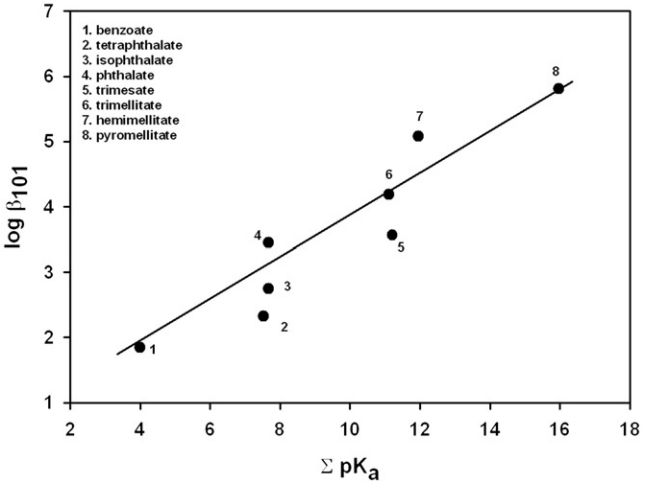

Figure 3. Correlation of log β_{101} with ΣpK_a.

Table 3. TRLFS data of the Cm(III) and Eu(III) with dicarboxylates; $[Cm(III)] = 2.0–4.0 \times 10^{-6}$ mol L^{-1}, $[Eu(III)] = 1.0 \times 10^{-4}$ mol L^{-1}; $T = 25°C$, $I = 0.1$ mol L^{-1} ($NaClO_4$).

	M : L ratio	pH	Excitation peak (nm)	Species	Lifetime (μs)	N_{H_2O} (±0.5)
Cm-HIDA	1 : 50	4.0	399.90	$Cm(HIDA)^+$	190 ± 10	4.8
	1 : 100	8.0	404.20	$Cm(HIDA)_2^-$	239 ± 5	1.8
	1 : 1000	6.0	404.20	$Cm(HIDA)_2^-$	253 ± 6	1.7
Eu-HIDA	1 : 4	4.0	579.24	$Eu(HIDA)^+$	204 ± 6	4.4
	1 : 8	6.0	580.08, 579.67, 579.97	$Eu(HIDA)_2^-$	502 ± 5	1.4
	1 : 20	8.0	580.11, 579.90	$Eu(HIDA)_2^-$	516 ± 3	1.3
Cm-MIDA	1 : 50	4.0	398.84	$Cm(MIDA)^+$	89 ± 4	6.4
	1 : 100	8.0	402.35	$Cm(MIDA)_2^-$	150 ± 6	3.4
Eu-MIDA	1 : 4	4.0	579.07	$Eu(MIDA)^+$	128 ± 5	7.5
	1 : 8	8.0	579.07, 579.34	$Eu(MIDA)^+$	177 ± 6	5.3
	1 : 20	6.0	579.51	$Eu(MIDA)_2^{2-}$	269 ± 8	2.7
Cm-EDDA	1 : 50	4.0	397.80	$Cm(EDDA)^+$	97 ± 3	5.8
	1 : 100	8.0	399.31	$Cm(EDDA)_2^-$	159 ± 4	3.2
Eu-EDDA	1 : 8	6.0	579.54	$Eu(EDDA)^+$	156 ± 8	5.6
			580.18	$Eu(EDDA)_2^-$	230 ± 8	3.8
	1 : 20	6.5	580.18, 579.54	$Eu(EDDA)_2^-$	221 ± 8	4.0
Cm-BDODA	1 : 1000	6.0	398.12, 394.89	$Cm(BDODA)^+$	118 ± 3	4.6
Eu-BDODA	1 : 4	4.0	578.77	$Eu(BDODA)^+$	178 ± 8	5.2
	1 : 20	6.0	–	$Eu(BDODA)_2^-$	275 ± 7	3.1
Cm-K21DA	1 : 800	5.0	399.65, 394.39	$Cm(K21DA)^+$	185 ± 5	2.6
	1 : 800	9.0	400.56, 394.42	Cm(K21DA)(OH)	413 ± 2	0.7
Eu-K21DA	1 : 1000	6.0	579.73	$Eu(K21DA)^+$	375 ± 8	2.1
Cm-K22DA	1 : 1000	5.0	398.26, 399.69, 401.54, 395.55	$Cm(K22DA)^+$	234 ± 3	1.9
		9.0	398.86, 400.48, 403.54, 395.77	Cm(K22DA)(OH)	490 ± 4	0.5
		11.5	398.86, 400.48, 403.54, 395.77	Cm(K22DA)(OH)	482 ± 6	0.5
Eu-K22DA		6.0	579.24, 579.79, 579.97	$Eu(K22DA)^+$	510 ± 6	1.4

via an oxygen atom from two carboxylates (Ln–O = 2.10 Å). In the 1 : 2 complex, metal–ether oxygen distances increase significantly (2.70 Å), indicating very weak interaction with metal in the center of the plane of the four oxygen donors from the four carboxylates by the perpendicular arrangement of the two ligands [7].

DPA and CA are reported to form 1 : 1, 1 : 2, and 1 : 3 complexes with Ln(III) cations [22]. CA has a coordination site like that of dipicolinic acid, but the increased aliphatic nature of CA decreases the stability and size selectivity of M(III) complexes. In the concentration range of our studies, formation of 1 : 1 and 1 : 2 complexes are observed. The stability constant values are listed in table 2 for Eu(III). The decreased stability of CA can be explained by a re-orientation of the OH– proton and coordination sites of the imino of the non-aromatic CA molecule, nitrogen inversion, which weakens the Ln–N coordination bond and decrease the stability of the complex compared to that of Ln–DPA. For comparison, the N_{H_2O} values of PA and PAO were measured. Formation of 1 : 1, 1 : 2, and 1 : 3 for PA and of the first two complexes for PAO was observed. Both PA and PAO displace 2.5 water molecules of hydration, reflecting bidentate coordination for these ligands in 1 : 1 and 1 : 2 complexation, while displacement of *ca* 1.3 water molecules of hydration by PA on the formation of the 1 : 3 complex indicates monodentate coordination in the 1 : 3 complex. The three peaks at 578.99, 579.25, and 579.50 nm, corresponding to the presence of 1 : 1, 1 : 2, and 1 : 3 complexes, are present in the spectrum of Eu-PA at an Eu : PA ratio of 1 : 1 and pH = 6.0 [23]. The N_{H_2O} values of 7.7, 6.7, and 5.8, respectively, indicate monodentate coordination for PA

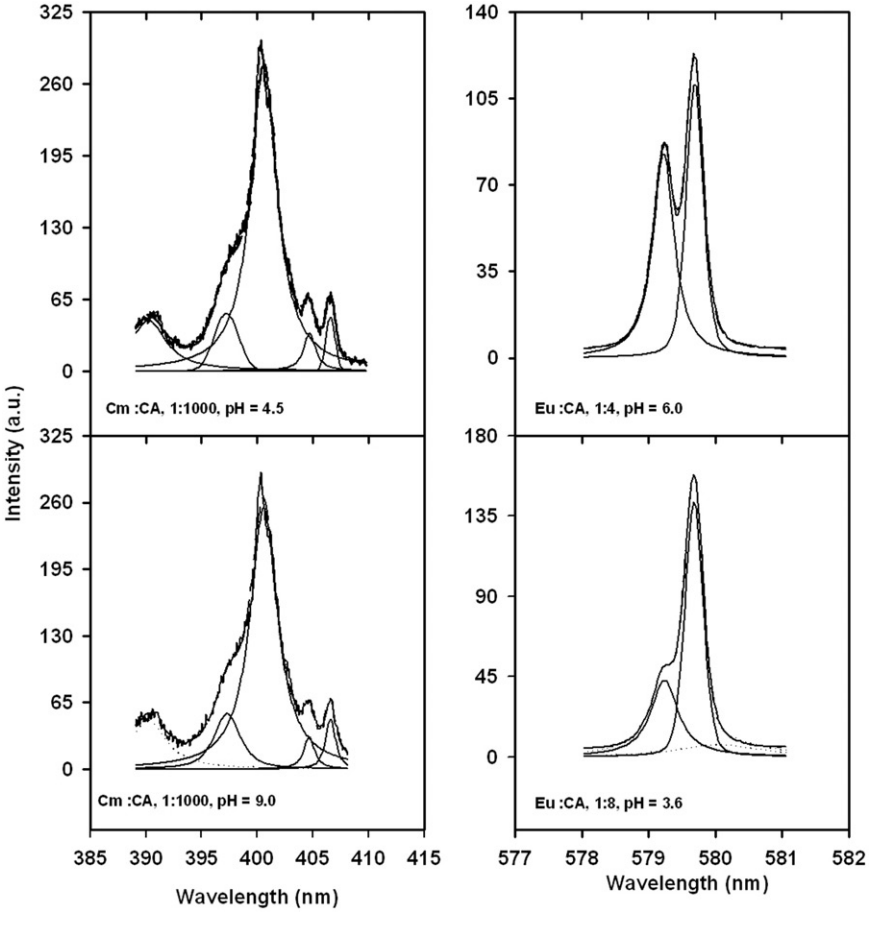

Figure 4. Excitation spectra of Cm-CA and Eu-CA; $[Cm^{3+}] = 4.0 \times 10^{-6}\,mol\,L^{-1}$; $Eu = 1 \times 10^{-4}\,mol\,L^{-1}$; $I = 0.1\,mol\,L^{-1}$ ($NaClO_4$), and $T = 25°C$.

[23]. With increased concentration of PA and pH = 6.0, bidentate coordination for PA (N is binding) is proposed [23].

The excitation spectra of Cm-CA and Eu-CA are shown in figure 4 and the measured N_{H_2O} values are listed in table 4. The removal of *ca* 3.0 water molecules of hydration indicates tridentate coordination for DPA and CA. The solid state structure of Gd–CA complex exists as a $Na_5Gd(CA)2(HCA)$ with 16 water molecules of hydration. Two CA molecules are completely deprotonated while one complex has a phenolic hydrogen. All three ligands are tridentate to the Gd(III) in a tricapped trigonal prismatic geometry [24]. The geometry of the ligands and that of the primary coordination sphere is very similar to that of Ho(DPA)(HDPA) [25]. However, those authors fail to mention how the hydrogen position was assigned and also state that water molecules were disordered. The phenolic proton could be reassigned as a proton of a water molecule that was hydrogen bonded to the CA, linking the $Gd(CA)_3$ units.

A single peak is observed at 397.69 nm for PDA complexation over the pH range 2–6. Eu-PDA has a peak at 578.94 nm which corresponds to a ligand coordination number,

Table 4. TRLFS data of the Cm(III) and Eu(III) with DPA, CA, PDTA, EGTA, and ENDADP; $[Cm(III)] = 2.0–4.0 \times 10^{-6}$ mol L^{-1}, $[Eu(III)] = 1.0 \times 10^{-4}$ mol L^{-1}; $T = 25°C$, $I = 0.1$ mol L^{-1} ($NaClO_4$).

M : L	Ratio	pH	Excitation peak (nm)	Species	Lifetime (μs)	N_{H_2O} (±0.5)
Cm-DPA	1 : 800	4.5	400.51	$Cm(DPA)^+$	100 ± 7	5.6
	1 : 800	9.0	405.02	$Cm(DPA)_2^{2-}$	148 ± 5	3.5
	1 : 800	11.0	406.83	$Cm(DPA)_3^{3-}$	540 ± 8	0.3
Eu-DPA	1 : 4	4.5	579.21	$Eu(DPA)^+$	150 ± 8	6.3
	1 : 8	6.0	579.68	$Eu(DPA)_2^{2-}$	276 ± 6	3.1
	1 : 100	8.0	580.25	$Eu(DPA)_3^{3-}$	1050 ± 5	0.3
Cm-CA	1 : 800	4.5	400.59	$Cm(CA)^+$	90 ± 3	6.3
	1 : 800	9.0	404.71	$Cm(CA)_2^{2-}$	184 ± 5	2.6
	1 : 800	11.5	406.60	$Cm(CA)_3^{3-}$	409 ± 7	0.7
Eu-CA	1 : 4	3.60	579.21	$Eu(CA)^+$	201 ± 6	4.5
	1 : 8	6.0	579.68	$Eu(CA)_2^{2-}$	292 ± 8	2.9
	1 : 100	8.0	580.21	$Eu(CA)_3^{3-}$	877 ± 15	0.5
Cm-PDA	1 : 800	6.0	397.69	$Cm(PDA)^{2+}$	81 ± 6	7.1
Eu-PDA	1 : 5	5.8	578.94	$Eu(PDA)^{2+}$	120 ± 8	8.0
Cm-PDTA	1 : 4	3.6	399.24, 402.06, 396.40	$Cm(PDTA)^-$	147 ± 5	3.5
	1 : 4	9.0	399.44, 402.00, 396.67	$Cm(PDTA)^-$	154 ± 6	3.3
Eu-PDTA	1 : 2	3.6	579.61, 580.11	$Eu(PDTA)^-$	348 ±	2.3
	1 : 2	9.0	579.61, 580.11	$Eu(PDTA)^-$	381 ±	2.0
	1 : 2	11.5	579.61, 580.10, 579.13	$Eu(PDTA)(OH)^{2-}$	498 ±	1.4
Cm-EGTA	1 : 4	3.6	404.74, 400.14, 395.62	$Cm(EGTA)^-$	271 ± 6	1.5
	1 : 4	9.0–11.5	399.23	$Cm(EGTA)^-$	266 ± 4	1.6
Eu-EGTA	1 : 2	3.6	580.05	$Eu(EGTA)^-$	680 ± 5	0.8
	1 : 2	9.0–11.5	580.05	$Eu(EGTA)^-$	666 ± 5	1.0
Cm-HDTA	1 : 800	4.2	–	$Cm(HDTA)^-$	122 ± 5	4.4
	1 : 800	9.2	–	$Cm(HDTA)(OH)^{2-}$	240 ± 5	1.8
Tb-HDTA*	1 : 2	10.4	–	–	–	3.0
Cm-ENDADP	1 : 800	4.2	402.31, 399.36, 396.28	$Cm(ENDADP)^-$	137 ± 3	3.9
	1 : 800	9.0	399.84	$Cm(ENDADP)(OH)^{2-}$	228 ± 4	1.9
Eu-ENDADP	1.2	3.6–8.0	–	$Eu(ENDADP)^-$	328 ± 8	2.5
Cm-PA	1 : 800	4.5	–	$Cm(PA)^{2+}$	85 ± 4	6.8
	1 : 800	7.0	398.84	$Cm(PA)_2^+$	129 ± 5	4.1
			400.21	$Cm(PA)_3$	178 ± 5	2.8
Eu-PA**	1 : 1	6.0	578.99	$Eu(PA)_2^{2+}$	136	7.7
	–	6.0	578.25	$Eu(PA)_2^+$	157	6.7
	–	6.0	579.50	$Eu(PA)_2^+$	181	5.8
	–	6.0	579.75	$Eu(PA)^{2+}$	210	5.0
	–	6.0	580.04	$Eu(PA)_2^+$	256	4.1
	–	6.0	580.29	$Eu(PA)_3$	362	2.9
Cm-PAO	1 : 800	4.2	–	$Cm(PAO)^{2+}$	88 ± 4	6.5
	1 : 800	6.0	–	$Cm(PAO)^+$	157 ± 4	3.2
Eu-PAO	1 : 3	4.2	–	$Eu(PAO)^{2+}$	187.5	4.9

*Ref. [31].
**Ref. [23].

CN_L, of 1.3 ± 0.5. Although the values were scattered due to the weak signal, the average values of the hydration of Cm(III) and Eu(III) calculated from repeated measurement of the luminescence lifetimes were 7.1 ± 0.5 and 8 ± 0.5, respectively. The peak position of the PDA species is the same as the value reported for the first acetate complexation ($EuAc^{2+} = 578.94$ nm), indicating that PDA is a weak complexant binding through a single carboxylate displacing one water molecule from the inner coordination sphere of Eu(III).

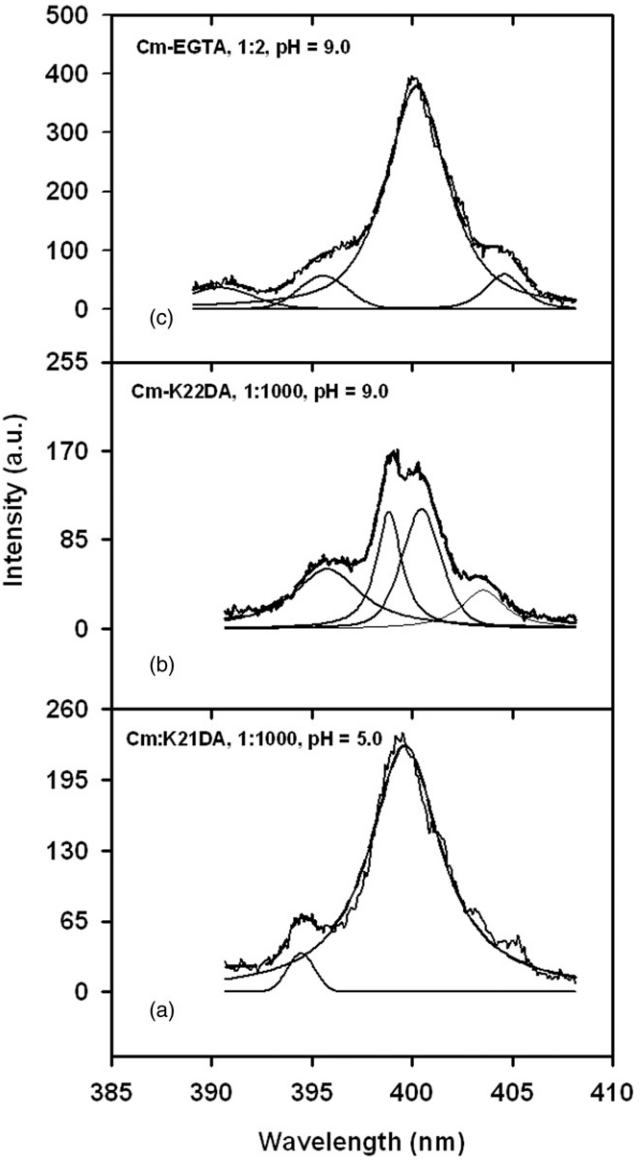

Figure 5. Excitation spectra of (a) Cm-K21DA; (b) Cm-K22DA, and (c) Cm-EGTA; $[Cm^{3+}] = 4.0 \times 10^{-6}$; $I = 0.1\,\text{mol}\,L^{-1}$ ($NaClO_4$), and $T = 25^{\circ}C$.

The cyclic ligands K21DA and K22DA and the open chain analog EGTA form 1 : 1 complexes as illustrated from linear curves of $1/D$ *vs.* $[L]^{n-}$ (figure 2(c), a representative graph for Cm-K22DA). The measured stability constant values of Cm(III), Am(III), and Eu(III) are listed in table 2 with values from the literature for comparison. The excitation spectrum of Cm-K21DA consists of a single band, while the spectra of Cm-K22DA and Cm-EGTA consist of two and three bands, respectively. The deconvoluted spectra of these complexes are shown in figure 5 and the calculated N_{H_2O}

values of the complexes are summarized in table 3. Luminescence data can be fitted to a single exponential decay, indicating fast chemical interchange between the species compared to that of the luminescence decay and the observed lifetime is a weighted average of the species present. The corresponding $^5D_0 \rightarrow {}^7F_0$ excitation spectra of Eu(III) show similar spectral patterns.

The lifetime data for $Cm(K21DA)^+$, $Cm(K22DA)^+$, and $Cm(EGTA)^-$ indicate that these complexes have *ca* 2.6, 1.9, and 1.5 water molecules of hydration, respectively. This difference in water molecules of hydration reflects coordination of ether oxygen atoms of K22DA to the metal cations. The appearance of multiple peaks for K22DA and EGTA and not for K21DA can be attributed to the bad fit of Eu(III) and Cm(III) within the macrocycle cavity of K22DA (cavity size $= 1.45 \pm 0.15$ Å *vs.* ionic radius of Cm(III) $= 1.09$ Å) [26] and of the noncyclic character of EGTA, plus the presence of extra carboxylic groups in EGTA. The Eu(III) with ionic radius of 1.05–1.25 Å (depending on coordination number) is better suited for K21DA (0.97 ± 0.13 Å). The stability constants (table 2) further reflect the importance of cavity size on complexation. For example, in the lanthanide series, Eu(III) forms the most stable complex with K21DA, while the larger Ce(III) forms the most stable complex with K22DA. An improper fit is a possible cause for the presence of multiple species. By contrast, EGTA is noncyclic with four carboxylates and has the ability to wrap around the metal ion, resulting in greater stability as compared to those of K21DA and K22DA complexes. With increased pH to 9.0 and 11.5, neither the spectra nor the lifetimes of Cm-EGTA or Eu-EGTA change. However, spectra and lifetime changes were observed for both of the macrocyclic complexes. The increased lifetimes are consistent with formation of ternary hydroxyl complexes; however, the shift of excitation bands to a lower wavelength with pH is in contrast to that expected for coordination of hydroxyl groups. Similar appearance of shorter wavelength peaks at higher pH were reported for Eu(III)–parvalbumin systems [27]. The ^1H and ^{13}C NMR data suggest long lived M–N and short lived M–O bonds for the Y-K21DA complex with $CN_T = 9.0$ (two carboxylate oxygen atoms, three ether oxygen atoms, two nitrogen atoms and two water molecules) [26]. For K22DA, the complex has a $CN_T = 9.0$ with one water molecule of hydration. Unlike K21DA, the M–N and M–O bonds are short lived for the K22DA complex and this complex undergoes fluctional processes that result in incomplete binding of the coordinating groups [26].

Polyaminotetracarboxylates PDTA, ENDADP, and HDTA form 1 : 1 complexes with the trivalent cations with strong stability constants (table 2 and figure 2(c), a representative graph for Cm-ENDADP and Am-ENDADP). The complexation strength of simple polyaminocarboxylates follows the order: CDTA (*trans*-1,2 diaminocyclohexane tetraacetate) > EDTA (ethylenediaminetetraacetate) > PDTA > ENDADP > HDTA [22]. An increase in the steric constraints of the polyaminocarboxylate, either by increasing the number of groups in the ligand backbone such as ENDADP in which two acetates are replaced by propionates or by increasing the number of groups in the ligand backbone such as HDTA, decrease the stability by *ca* 3–8 log units (table 2) [22]. The addition of ether functionalities (EGTA) or of an additional aminocarboxylate (DTPA) increases the stability constants by 3–5 log units as compared to EDTA. Replacement of one or two carboxylates of DTPA by amide functionalities or sugar groups such as DTPA-MA, DTPA-BMEA, and DTPA-BGAM result in complexes with much lower stability constants ($\log \beta_{101} \sim 18$ and ~ 16, table 2) than DTPA ($\log \beta_{101} \sim 22$). Like polyaminotetracarboxylates, all these ligands form 1 : 1

complexes (figure 2(d), a representative graph for Cm-BMEA and Cm-BGAM). The similarity in the stability constant values of DTPA-BMEA and DTPA-BGAM (table 2) with these cations implies that incorporation of bulky sugar groups has not altered significantly the nature and strength of complexation. NMR data (^{1}H and ^{13}C) support octadentate coordination *via* three carboxylate oxygen atoms, three nitrogen atoms, and two amide oxygen atoms [28]. Introduction of functional groups on the ethylenediamine backbone as in N-methyl-MS-325 also reduces the stability of the complexes compared to that of DTPA. This may be explained by the steric effect of the bulky substituents constraining the ligands *via* chelation. The stability of DTPA-derivative ligands follows the order: DTPA > N-methyl-MS-325 > DTPA-MA > DTPA-BMEA≈DTPA-BGAM.

Cm complexes of PDTA and ENDADP contain *ca* 3.5 water molecules of hydration. Since this value is the same as those for EDTA and PDTA complexes, it can be concluded that acetate and propionate groups have the same effect on M(III) coordination (table 4). For Cm-EDTA, the existence of two peaks in spectra of Cm-PDTA/ENDADP and Eu-PDTA/ENDADP (figure 6) are indicative of the presence of two different species with two and three water molecules of hydration. The third peak in the spectra at *ca* 396.00 nm (figure 6) is due to large ligand field splitting by the stronger metal–ligand interaction [29]. At pH > 9.0, the two peaks have the same position for the PDTA complexes, while only one peak is observed for Cm-ENDADP. The increased average lifetime indicates the formation of the ternary hydroxyl complex for both these ligands $Cm(L)(OH)^{2-}$ (L = PDTA and ENDADP). The N_{H_2O} values of PDTA and ENDADP complexes are consistent with $N_{H_2O} = 3.9$ for Cm-EDTA [6], indicating hexadentate coordination for both ligands. Hexadentate coordination of EDTA is supported by X-ray diffraction studies [30]. Structure variation across the Ln-series has been observed with complexes nine-coordinate for the larger, lighter lanthanides and eight-coordinate for heavier, smaller lanthanides. Extra methylene groups in the ligand backbone displace no extra water molecules of hydration from the inner coordination shell of the metal cations. For example $N^{-}_{H_2O,\,Eu(EDTA)} = 2.7$ (n = number of methylene groups = 2), $N^{-}_{H_2O,\,Eu(TMDTA)} = 2.4$ ($n = 3$) and $N^{-}_{H_2O,\,Eu(HDTA)} = 3.0$ ($n = 6$) are essentially the same. However, their complexation strengths decrease with increase in n, $Eu(EDTA)^{-}$, $\log \beta_{101} = 16.23$, $I = 0.5\,mol\,L^{-1}$, $Eu(TMDTA)^{-}$ (TMDTA = trimethylenediamine tetraacetate), $\log \beta_{101} = 13.54$, $I = 0.1\,mol\,L^{-1}$, and $Eu(HDTA)^{-}$, $\log \beta_{101} = 9.27$, $I = 1.0\,mol\,L^{-1}$ [22] reflecting decreased stability of the chelate ring from five (EDTA), six (TMDTA) to nine (HDTA). A dimeric structure has been proposed for Eu-HDTA with each metal cation binding *via* two carboxylate oxygen atoms and a nitrogen atom from each ligand plus three water molecules [31].

Complexes of EGTA, DTPA, and their derivatives have only one water molecule of hydration attached to the metal (table 5). Non-integral number of coordinated water molecules suggests the presence of species with different extents of hydration in dynamic equilibrium. Since interchange between the different states is fast on the luminescence time scale, the measured hydrations represent average values. The NMR and solid state structure analysis of $Nd(EGTA)^{-}$ and $Er(EGTA)^{-}$ are consistent with the presence of one water molecule with short lived M–O and M–N bonds. The smaller lanthanides (La to Sm) display a rapid equilibrium between CN_T of 10 and 9, while lanthanides from Eu to Tm between CN_T of 9 and 8 with EGTA binding *via* four carboxylate oxygen atoms, two ether oxygen atoms and two nitrogen atoms. The four

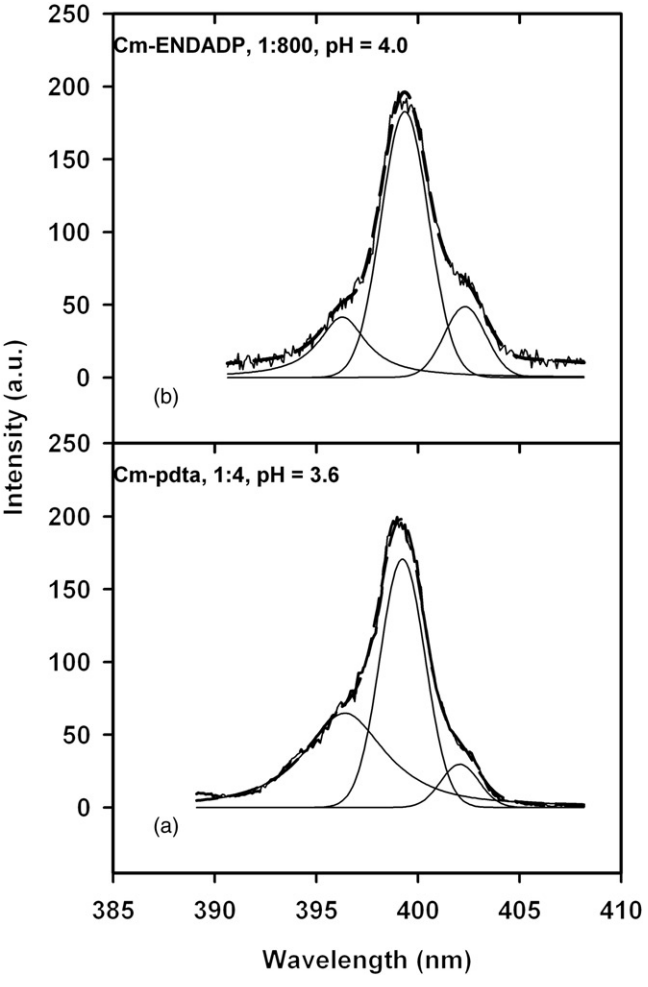

Figure 6. Excitation spectra of Cm-PDTA and Cm-ENDADP; $[Cm^{3+}] = 4.0 \times 10^{-6}$; $I = 0.1\,mol\,L^{-1}$ ($NaClO_4$), and $T = 25°C$.

peaks in spectra of Cm-N-methyl-MS-325 indicate the presence of small amounts of other forms of the complex with two water molecules of hydration (figure 7). However, for Eu-N-methyl-Ms-325, a sharp peak at 579.88 nm indicates no such structural heterogeneity. Four peaks are also present in excitation spectra of Cm-DTPA-BMEA, Cm-DTPA-BGAM, and Cm-DTPA-MA (figure 7). The lifetime and N_{H_2O} values indicate octadentate coordination for all these ligands. The similarities of ^1H NMR spectra of Lu-DTPA-BMEA and Lu-DTPA further support similar structures.

Macrocyclic aminopolycarboxylates such as DOTA form 1 : 1 complexes with these cations with enhanced stability constant values with respect to analogous acyclic aminopolycarboxylates. The enhanced stability of the DOTA complexes reflects kinetic inertness due to the encapsulating nature of the macrocyclic ligands (macrocyclic or clathrochelate), and thermodynamic stabilization due to the large degree of

Table 5. TRLFS data of the Cm^{3+} and Eu^{3+} with linear and cyclic polyaminocarboxylates; $[Cm(III)] = 2.0–4.0 \times 10^{-6}$ mol L^{-1}, $[Eu(III)] = 1.0 \times 10^{-4}$ mol L^{-1}; $T = 25°C$, $I = 0.1$ mol L^{-1} ($NaClO_4$).

	Ratio	pH	Excitation (nm)	Species	Lifetime (μs)	N_{H_2O} (±0.5)
Cm-DTPA-MA	1 : 4	4.0	400.26, 395.66, 391.30	$Cm(DTPA\text{-}MA)^-$	252 ± 5	1.7
	1 : 4	9.0–11.5	400.26, 395.66, 391.30	$Cm(DTPA\text{-}MA)^-$	276 ± 15	1.5
Eu-DTPA-MA	1 : 5	4.0	579.95	$Eu(DTPA\text{-}MA)^-$	709 ± 10	0.8
	1 : 5	9.0–11.5	579.95	$Eu(DTPA\text{-}MA)^-$	715 ± 6	0.8
Cm-DTPA-BMEA	1 : 4	3.6	403.74, 400.32, 395.90, 390.78	Cm(DTPA-BMEA)	266 ± 6	1.6
	1 : 4	9.0–11.5	403.75, 400.42, 395.65, 390.72	Cm(DTPA-BMEA)	260 ± 8	1.6
Eu-DTPA-BMEA	1 : 4	3.6	579.95	Eu(DTPA-BMEA)	653 ±10	0.9
	1 : 4	9.0–11.5	579.95	Eu(DTPA-BMEA)	653 ± 11	0.9
Cm-DTPA-BGAM	1 : 4	3.6	404.44, 400.42, 395.63, 391.49	Cm(DTPA-BGAM)	260 ± 8	1.6
	1 : 4	9.0–11.5	404.44, 400.42, 395.63, 391.49	Cm(DTPA-BGAM)	363 ± 10	0.9
Eu-DTPA-BGAM	1 : 2	3.6	579.95	Eu(DTPA-BMEA)	571 ± 5	1.2
	1 : 2	9.0–11.5	579.98	Eu(DTPA-BMEA)	704 ± 10	0.8
Cm-NMS-325	1 : 800	3.6–9.0	404.30, 400.38, 399.47, 396.19	$Cm(NMS\text{-}325)^-$	181 ± 10	2.6
	1 : 800	13.0	404.30, 400.38, 399.47, 396.19	$Cm(NMS\text{-}325)^-$	151 ± 6	3.4
Eu-NMS-325	1 : 2	3.6	579.88	$Eu(NMS\text{-}325)^-$	373 ± 5	2.1
	1 : 2	9.0–11.5	579.88	$Eu(NMS\text{-}325)^-$	374 ± 4	2.1
Cm-DOTA	1 : 800	5.0	404.78, 403.28, 401.94, 400.74, 399.57, 396.69	$Cm(DOTA)^-$	285 ± 6	1.4
	1 : 800	9.0–11.5	404.78, 403.28, 401.94, 400.74, 399.57, 396.69	$Cm(DOTA)^-$	270 ± 4	1.5
Eu-DOTA			579.81	$Eu(DOTA)^-$	552 ± 10	1.2

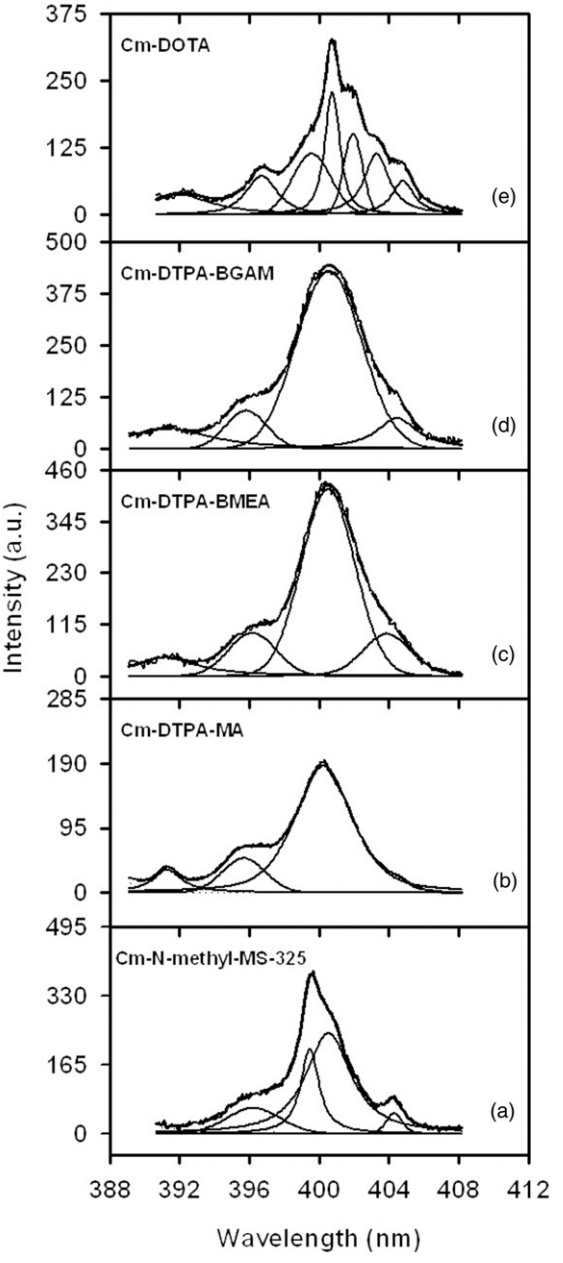

Figure 7. Excitation spectra of (a) Cm : N-methyl-MS-325, 1 : 2, pH = 9.0; (b) Cm : DTPA-MA; 1 : 2, pH = 9.0; (c) Cm : DTPA-BMEA, 1 : 2, pH = 9.0; (d) Cm : DTPA-BGAM, 1 : 2, pH 9.0, and (e) Cm : DOTA, 1 : 2, pH = 9.0 $[Cm^{3+}] = 4.0 \times 10^{-6}$; $I = 0.1\ mol\ L^{-1}$ ($NaClO_4$), and $T = 25°C$.

preorganization of the ligand. Excitation spectra of Cm-DOTA show seven peaks indicating structural heterogeneity (figure 7). The peaks at lower wave number are due to the large ligand field splitting by the stronger metal–ligand interaction [29]. For Eu-DOTA a single peak at 579.81 nm indicates no structural heterogeneity.

Luminescence lifetime data of Cm-DOTA and Eu-DOTA indicate an N_{H_2O} of *ca* 1.0. Solid-state structure analysis of $Eu(DOTA)^-$ indicates that the chelate is strained, due to the poor fit of Eu(III) into the DOTA ring, resulting in variable Eu–N bond lengths. The presence of a water molecule of hydration indicates binding *via* four nitrogen atoms and four oxygen atoms in square antiprismatic geometry [32]. The smaller, heavy lanthanides form stronger chelates, because the diameter of the metal ion provides a better fit to the cavity size of DOTA [32]. Structural variation across the Ln-series was observed for the macrocyclic DOTA complex [33]. The X-ray crystal structure determinations of six Ln(DOTA) (Ln = Ce, Pr, Nd, Dy, Tm, and Sc) complexes indicate significant shrinkage of all M–N and M–O distances (*ca* 0.2) in $Tm(DOTA)^-$ as compared to that of $Ce(DOTA)^-$ [34]. Discussions based on the TRLFS studies are qualitative and the hydration number data alone do not provide compelling evidence on the structure of these complexes. Further, studies on crystal structures, NMR, and EXAFS could provide more insight into the structures of these complexes.

4. Conclusion

Both the decay constants and the stability constant measurements indicate that under conditions of this study, TMA, HMA, PMA, and TSA form only 1 : 1 complexes, while PHA, PA, and PAO form both 1 : 1 and 1 : 2 complexes. Stability constants of the 1 : 1 complexes show linear correlation with the basicity of the ligand and their complexation strength follows the order: PHA∼TSA > TMA > PMA > HMA. The carboxylates with adjacent carboxylates are bidentate and replace two water molecules of hydration upon complexation; displacement of 1.5 water molecules of hydration by TSA indicates greater binding capability of this ligand due to contributions from the non-bonding carboxylates. The dicarboxylates MIDA, HIDA, EDDA, and BDODA form both 1 : 1 and 1 : 2 complexes. The stability constant of 1 : 1 complexes follows the trend: HIDA > EDDA > IDA(iminodiacetate) ≈ MIDA > BDODA. Complexes of M-MIDA are tridentate, while M-HIDA is tetradentate in both the 1 : 1 and 1 : 2 complexes. Due to steric hindrance, the M-BDODA and M-EDDA complexes are tetradentate in the 1 : 1 and bidentate in the 1 : 2 complexes. The macrocyclic dicarboxylates K21DA and K22DA form 1 : 1 complexes. The hydration data indicate two and one water of hydration in these complexes, respectively. DPA and CA are tridentate in 1 : 1, 1 : 2, and 1 : 3 complexes.

Simple polyaminocarboxylates PDTA and ENDADP, like EDTA, are hexadentate with *ca* 3.5 water molecules of hydration. Polyaminocarboxylates with additional functional groups in the ligand backbone (EGTA and HDTA) or with additional number of groups in the carboxylate arms DTPA-MA, DTPA-BMEA, and DTPA-BGAM are octadentate with one water molecule of hydration, except N-methyl MS-325, which is heptadentate with two water molecules of hydration and HDTA which is probably dimeric with three water molecules of hydration. The addition of ether functionalities (EGTA) or of an additional aminocarboxylate (DTPA) increases the stability constants by 3–5 log units as compared to EDTA. The replacement of one or two carboxylates of DTPA by amide functionalities or sugar groups (DTPA-MA, DTPA-BMEA, and DTPA-BGAM) results in complexes with much lower stability

constants. The stability of DTPA-derivatives follows the order: DTPA > N-methyl-MS-325 > DTPA-MA > DTPA-BMEA ≈ DTPA-BGAM.

Complexes of macrocyclic ligands K22DA and DOTA have one water molecule of hydration, while K21DA complexes have two water molecules. These data give insight into the role of the steric effect on hydration of the cations. The composition of the complexes of Cm(III) and Eu(III) are the same. The hydration number of Cm(III) in these complexes is larger than that of Eu(III) because of larger average coordination number of Cm(III) (*ca* 0.5 units larger) compared to Eu(III) with polyaminocarboxylates.

Acknowledgments

The support of this work by the US Department of Energy, Office of Basic Energy Science, is gratefully acknowledged.

References

[1] G.R. Choppin. *J. Less-Common Met*., **112**, 193 (1985).
[2] R.M. Smith, A.E. Martell. *Sci. Total Environ*., **64**, 125 (1987).
[3] J.V. Beitz, J.P. Hessler. *Nucl. Technol*., **51**, 169 (1980).
[4] A. Barkleit, G. Geipel, M. Acker, S. Taut, G. Bernhard. *Spectrochim. Acta, Part A*, **78**, 549 (2011).
[5] N.M. Edelstein, R. Klenze, T. Fanghanel, S. Hubert. *Coord. Chem. Rev*., **250**, 948 (2006).
[6] T. Kimura, G.R. Choppin. *J. Alloys Compounds*, **213/214**, 313 (1994).
[7] G.R. Choppin, E.N. Rizkalla. In *Handbook on the Physics and Chemistry of Rare Earths*, K.A. Gschneidner Jr, L. Eyring, G.R. Choppin, G.H. Lander (Eds), Vol. 18, Elsevier Science, North-Holland, Amsterdam, The Netherlands (1994).
[8] S. Skanthakumar. *Inorg. Chem*., **46**, 3845 (2007).
[9] G. Tian, N.M. Edelstein, L. Rao. *J. Phys. Chem. A*, **115**, 1933 (2011).
[10] P. Lindqvist-Reis, R. Klenze, G. Schubert, T. Fanghanel. *J. Phys. Chem. B*, **109**, 3077 (2005).
[11] H. Wimmer, J.I. Kim. Report RCM 00992. Institut Fur Radiochemie, Technische Universitat Munchen, Garching, pp. 234 (1992).
[12] F.S. Richardson. *Chem. Rev*., **82**, 541 (1982).
[13] J.C.G. Bunzli, In *Lanthanide Probes in Life, Chemical and Earth Sciences*, J.C.G. Bunzli and G.R. Choppin (Eds), Elsevier, Amsterdam, p. 219 (1989).
[14] T. Kimura, G.R. Choppin, Y. Kato, Z. Yoshida. *Radiochim. Acta*, **72**, 61 (1996).
[15] A.B. Busov, V.P. Shilov. *Radiochemistry*, **41**, 1 (1999).
[16] K.M. Schaab. PhD dissertation thesis, The Florida State University (1998).
[17] Z.M. Wang, L.J. van de Burgt, G.R. Choppin. *Inorg. Chim. Acta*, **293**, 167 (1999).
[18] G.R. Choppin, Z.M. Wang. *Inorg. Chem*., **36**, 249 (1997).
[19] L. Zekany, I. Nagypal, D. Leggett (Eds). *Computational Methods for the Determination of Stability Constants*, Plenum Press, New York (1985).
[20] P. Gran, A. Sabatini, A. Vacca. *Talanta*, **43**, 1739 (1996).
[21] S. Lis, G.R. Choppin. *J. Alloys Compounds*, **225**, 257 (1995).
[22] A.E. Martell, R.M. Smith, R.J. Motekaites. *NIST Critically Selected Stability Constants of Metal Complexes*, Version 7.0, Texas A&M University, TX, USA (2003).
[23] Y.J. Park, B.H. Lee, W.H. Kim, Y. Do. *J. Colloid Interface Sci*., **209**, 268 (1999).
[24] A.K. Hall, J.M. Harrowfield, B.W. Skelton, A.H. White. *Acta Cryst. C*, **C56**, 407 (2000).
[25] A. Fernandes, J. Jaud, J. Dexpert-Ghys, C. Brouca-Cabarrecq. *Polyhedron*, **20**, 2385 (2001).
[26] R.C. Holz, S.L. Klakamp, C.A. Chang, W.D. Horrocks Jr. *Inorg. Chem*., **29**, 2651 (1990).
[27] M.T. Henzl, R.E. Birnbaum. *J. Biol. Chem*., **263**, 10674 (1988).
[28] H. Imura, G.R. Choppin, W.P. Cacheris, L.A. de Learie, T.J. Dunn, D.H. White. *Inorg. Chim. Acta*, **258**, 227 (1997).

[29] M. Weigl, M.A. Denecke, P.J. Panak, A. Geist, K. Gompper. *J. Chem. Soc., Dalton Trans.*, 1281 (2005).
[30] J. Wang, P. Hu, B. Liu, X. Jin, Y. Kong, J. Gao, D. Wang, B. Wang, R. Xu, X. Zhang. *J. Coord. Chem.*, **63**, 2193 (2010).
[31] S. Lis, J. Konarski, Z. Hnatejko, M. Elbanowski. *J. Photochem. Photobiol. A*, **79**, 25 (1994).
[32] M.R. Spirlet, J. Rebizant, J.F. Desreux, M.F. Loncin. *Inorg. Chem.*, **23**, 359 (1984).
[33] W.P. Cacheris, S.K. Nickle, A.D. Sherry. *Inorg. Chem.*, **26**, 958 (1987).
[34] F. Benetollo, G. Bombieri, L. Calabi, S. Aime, M. Botta. *Inorg. Chem.*, **42**, 148 (2003).
[35] V.K. Manchanda, P.K. Mohapatra. *Polyhedron*, **9**, 2455 (1990).
[36] C.A. Chang, Y.H. Chen, H.Y. Chen, F.K. Shieh. *J. Chem. Soc., Dalton Trans.*, 3243 (1998).